Payload Designer

A design tool for the FINCH Eye payload

Software Design Description

Built by
FINCH Payload Team
Space Systems Division
University of Toronto Aerospace Team

Updated December 2021

Contents

0 Revision History **3**

1 Introduction **4**

2 Design Values **4**
2.1 Modularity . . . 4
2.2 Usability . . . 4
2.3 Traceability . . . 4

3 Functional Requirements **5**

4 Scope & Limitations **5**

5 Platform **5**

6 System Architecture **6**
6.1 Components . . . 6
6.1.1 Vectorization . . . 6
6.2 Pipelines . . . 7

7 Data Design **7**

8 Project Stages **7**

9 Workflow **8**

10 Optimization **8**

11 Interoperability with Broketran **8**

A Foreoptics Model **10**
A.1 Aperture Diameter . . . 11
A.2 Effective Focal Length . . . 11
A.3 Telecentricity . . . 11
A.4 Magnification . . . 11
A.5 Numerical Aperture . . . 11
A.6 Minimum Back Focal Length . . . 11
A.7 F/value (f/number) . . . 11
A.8 Geometric Etendue . . . 11
A.9 Flux . . . 12

B Slit Model **12**
B.1 Image Width . . . 13
B.2 Slit Width . . . 13

C Lens Models **13**
C.0 Thin Singlet Lens Model . . . 13
C.0.1 Image distance . . . 14
C.0.2 Source distance . . . 14
C.0.3 Image height . . . 15
C.0.4 Source Height . . . 15
C.1 Focal length . . . 15
C.1.1 Magnification . . . 15
C.2 Thick Singlet Model . . . 15
C.2.1 Position of the principal planes . . . 16
C.2.2 Focal length . . . 16
C.2.3 Image distance from principal plane . . . 17
C.2.4 Image distance from focal point . . . 17
C.2.5 Image height . . . 17

C.3 Achromatic Doublet Model . . . 17
C.3.1 Choosing materials for each lens . . . 18
C.3.2 Calculating focal lengths of lens pair . . . 18
C.3.3 Calculating effective focal length . . . 19
C.3.4 Calculating radius of curvature . . . 19

D Dichroic Bandpass Filter Model **19**
D.1 Incident Beam . . . 19
D.2 Transmitted Beam . . . 20

E Diffractor Models **20**
E.1 Surface-Relief Grating Model . . . 20
E.1.1 Dispersion . . . 21
E.1.2 Resolving Power and Spatial Resolution . . . 21
E.2 VPH Grating Model . . . 21
E.3 VPH Grism Model . . . 22
E.3.1 Angular distribution of diffracted wavelengths . . . 23
E.3.2 Undeviated wavelength . . . 24
E.3.3 Diffraction Efficiency . . . 24
E.3.4 Resolvance . . . 25
E.3.5 Resolution . . . 26

F Sensor Model **26**
F.1 Signal-to-Noise . . . 26
F.2 Frequency-Based Signal-to-Noise . . . 27

G Scrap **27**

0 Revision History

Version	Date	Changes	Authors
0.1	2021-12-30	Document structured & objectives laid out	David Maranto, Shiqi Xu
1.0	2022-01-14	Component models fully drafted up	Entire project team [1]
1.1	2022-01-16	Component models reviewed	Shiqi Xu, David Maranto

[1] Members: Ginny Guo, Jennifer Zhang, Eman Shayeb, Stephanie Lu, Kejsi Gjerazi, Amy Saranchuk, David Maranto, Shiqi Xu

1 Introduction

We present a software design document for the **payload designer** (hereafter referred to as the `program`): a high-level parametric design tool for the FINCH Eye hyperspectral imaging payload being developed by the University of Toronto Aerospace Team.

The objectives of the document are as follows:

- Outline all parts of the software and how they will work in a cohesive system architecture.
- Address various design concerns and describe rationales for the adopted solutions.
- Act as a stable reference over the course of development.
- Coordinate the developer team under a single vision.

In other words, formally document all rough work including research, equations, references, and software design decisions. The development of such a tool is motivated by the payload team's need to arrive at refined component-specific requirements. As we have been finding through correspondence with component manufacturers, there are many component parameters that cannot be estimated from reference designs and rule-of-thumb estimates alone. Many are very much instrument-specific, and depend on the scientific objectives as well as many other coupled factors in the system. Attempts at modelling various aspects of the payload have been made (see the Optics Toolkit[2]). These tools have sufficed for the first few design iterations of the payload (up to FINCH Eye v2) but have largely been disjoint and under-documented. Now that the payload team is entering the final stages of design, however, a more formal approach is warranted: one that enables a unified analysis of the entire payload and all of its components. This is the vision for the payload designer.

Source code for the project can be found on Github.

2 Design Values

The following design values guide the design of the `program`.

2.1 Modularity

The adopted software system architecture strives to enable as much modularity and configurability as necessary to enable whatever types of analyses and tradeoff studies are desired. Component models are implemented using object-oriented programming (OOP) to leverage the modularity of the paradigm. Similar components may inherit properties of a parent component (i.e. a VPH grating class may inherit methods and attributes from the surface-relief grating class). This reduces redundancy and the potential for buildup of technical debt.

2.2 Usability

The `program` strives to let the designer focus on the design as opposed to acting as a hindrance from it. Configuration of design parameters is simple, allowing for rapid iteration, with little to no need to get into the gritty details of the implementation. The method used to construct new analyses is straightforward and intuitive. Outputs are reported in a user-friendly format, and leverage multi-dimensional visualization tools.

2.3 Traceability

The `program` and its supporting documentation strive to be traceable. This means all equations and mathematical derivations are traceable back to a *source*, along with proper description of all assumptions associated with a particular model. This level of transparency is part of proper engineering practice as we mature the design of the payload.

[2] Powered by Desmos, mankind's greatest invention. Second only to Python.

3 Functional Requirements

Requirement language is to be interpreted as described in RFC 2119.

The `program` ...

i. Must enable calculation of any quantity of interest associated with the payload given the parameters that define the quantity.

ii. Must allow for visualization of the parameter space for a given quantity to enable trade-off analyses.

iii. Should allow for automatic optimization of a quantity of interest given a parameter space and constraints.

iv. May expose controls and display results to a user-interface.

4 Scope & Limitations

The following defines the scope of what the `program` intends to be and what it is not. A well-defined scope for the project is necessary to ensure the primary objectives of the project are met within the time constraints, and to avoid the development of functionality that may be redundant in the context of the other pre-existing tools available to the optics team.

- **Closed-form equations**: All the equations that are used to model the payload system are closed-form. First- and/or second-order approximations are acceptable. Consideration of higher-order phenomena such as optical aberrations is better left to detailed simulations in CODE V[3]
- **Ray tracing**: the `program` will **not** conduct ray tracing. While a ray tracing engine would allow for the direct coupling of mechanical constraints with the system parameters, this is again better left to CODE V. The `program` is intended to be a high-level design tool. In effect, this limits the types of physical parameters that can be solved for to angles and relative distances.

5 Platform

The `program` is to be developed as a Python application. A number of development environments and platforms were considered. The rationale for converging on Python is traced below.

- **Desmos:** High interactability with built-in sliders and plotting interface. High-fidelity visualization is possible, but requires considerable time investment to do right. Matrix algebra is possible, but requires some hacky solutions to implement. Quickly becomes cluttered and hard to document with more complex programs.
- **GeoGebra:** Big sister to Desmos. Matrix algebra is built-in, but same arguments of clutter and complexity apply as Desmos.
- **Google Colab:** Benefits of Python, plus sliders and other interactive UI elements easily creatable via markdown. Linear top-down structure may be limiting with respect to MathCAD.
- **GSOLVER:** Would produce the most accurate representation of our grating characteristics. Is only useful in the context of diffractor design, and may be excessive for our purposes. We should be alright with first- and second-order approximations of our diffractor models.
- **MathCAD:** Non-linear project structure makes for a more flexible development environment. Free version is very limited, and does not allow access to symbolic manipulation engine. Paid version is paid.
- **MATLAB:** Supports vectorization out of the box. MATLAB apps with a UI can be made fairly easily with sliders and plots, but the language is terrible. Period. MATLAB apps are nice, but can quickly become limiting compared to Python.

[3]CODE V is the optic team's optical simulation tool.

- **Python:** Greatest flexibility in most respects. `Numpy` allows for vectorized functions. Can pair with `Tkinter` or `Pygame` to produce UI. Nice graphs are possible using `Plotly`. No support for function overloading. UI development is not as straightforward as a MATLAB app.
- **Unity:** Language supports function overloading. Would require team to learn C#. Building the payload designer on top of an entire game engine may be excessive, and not at all lightweight to run and develop on.

✓ *Recommendation: a Python application, with the potential for adding user-interactability through notebooks built using IPython in Google Colab.*

6 System Architecture

From a system architecture perspective, the payload designer can be seen as a collection of component models strung together in various arrangements or *pipelines*. We describe component models and pipelines in turn.

6.1 Components

Component models are implemented as classes (see Python documentation), possessing attributes that define the parameters of the component, alongside methods that enable the calculation of attributes that are not initially defined.

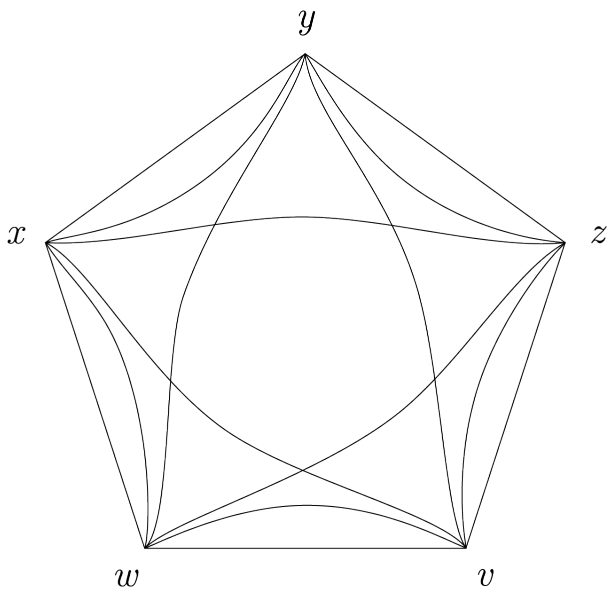

Figure 1: Component class architecture.

Where v, w, x, y, and z are attributes defining the component. Connecting lines are methods used to compute an attribute given the other attributes it depends on. It should be noted that not every parameter is necessarily dependent on every other parameter which defines the component. The concept of input and output variables is dropped in favour of a general multi-directional dependency approach. This is done to provide the design team with as much flexibility as possible in their analysis. For example, a designer wishing to know the associated signal-to-noise ratio (SNR) for a particular slit width might build a pipeline that computes SNR as a function of slit width and all other required parameters. At a later time, the designer may wish to know the slit width required to reach a particular SNR target. To accomplish this, they would simply do some rewiring of the components in the pipeline. The internal logic of the component classes would adjust accordingly to compute slit width as a function of SNR.

6.1.1 Vectorization

6.2 Pipelines

A pipeline refers to a collection of components wired together to produce some output(s).

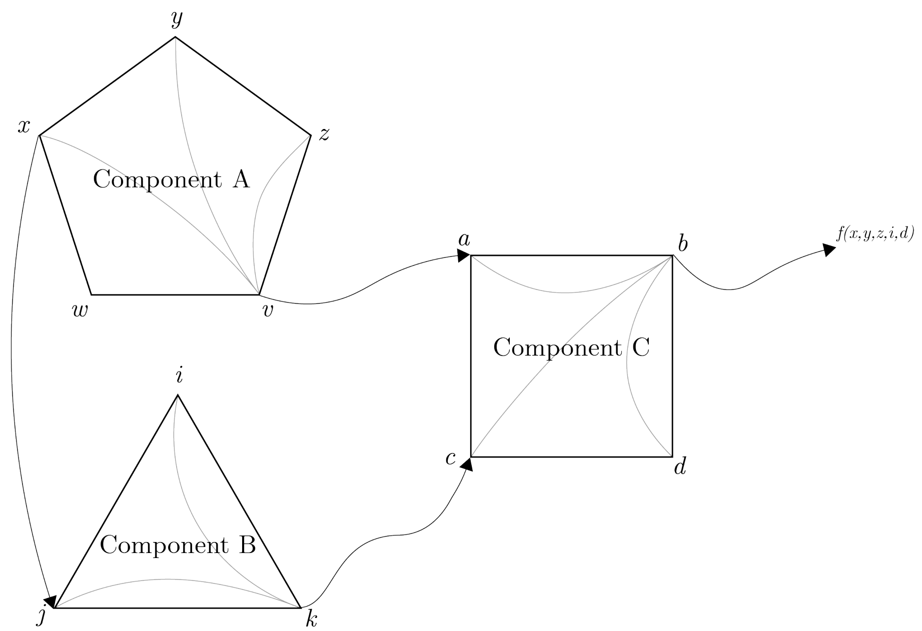

Figure 2: A generic pipeline architecture.

Practically, a pipeline is implemented in the following manner:

Algorithm 1 Component pipeline to solve for parameter b. A, B, and C are component classes.

Require: x, y, z, i, d

$\triangleright$ component instantiation

$A.x \leftarrow x$
$A.y \leftarrow y$
$A.z \leftarrow z$
$B.i \leftarrow i$
$C.d \leftarrow d$

$\triangleright$ pipeline definition and propagation

$j \leftarrow A.x$
$a \leftarrow A.v()$
$c \leftarrow B.k(j)$
$b \leftarrow C.b(a, c)$
return b

7 Data Design

David

8 Project Stages

The project is defined in four stages. These are:

- **Stage 0**: Functional requirements are defined. Proposed system architecture is prototyped and validated. Developers are onboarded onto the payload designer development team and are familiarized with the toolchain.
- **Stage A**: Mathematical models for components are defined.

- **Stage B**: Components are implemented in source code. Visualization and optimization tools are implemented.
- **Stage C**: Numerical analysis and tradeoff studies begin. The component selection team defines component-specific requirements from findings. Parameters are validated and refined by the optical simulations team.

9 Workflow

The workflow for the development of component models (Stages A & B) is described:

1. A literature review is conducted on a specific component to source relevant parameters, equations, and typical values for the parameters that describe the component.
2. A mathematical model created and presented in this document. Any required derivations are made and presented. The assumptions and limitations of the model are noted.
3. Once the mathematical model for the component is peer-reviewed, it is implemented in the project source code.
4. Unit tests are written to validate the functionality of the component class.

10 Optimization

Eman, David

The parametric architecture of the payload designer enables optimization. Optimization is a key part of any design process. The optimization strategies and systems adopted are described.

11 Interoperability with Broketran

David, Harshit

References

[1] Victor Argueta. *Achromatic Doublet Design And Optimization*. https://www.opticsforhire.com/blog/achromatic-doublet-with-flint-crown-glass. Accessed: 2022-01-09.

[2] Samuel C Barden, James A Arns, and Willis S Colburn. "Volume-Phase Holographic Gratings and Their Potential for Astronomical Applications." In: *Proceedings of SPIE - The International Society for Optical Engineering* 3355 (July 1999).

[3] Samuel C Barden et al. "Volume-Phase Holographic Gratings and the Efficiency of Three Simple Volume-Phase Holographic Gratings." In: *Publications of the Astronomical Society of the Pacific* 112.772 (2000), pp. 809–820.

[4] Boundless. *Lenses*. en. https://courses.lumenlearning.com/boundless-physics/chapter/lenses/. Accessed: 2022-1-10.

[5] *Coupling into your spectrometer*. https://ibsen.com/wp-content/uploads/Coupling-into-your-spectrometer.pdf. Accessed: 2022-01-01.

[6] *DevOptical Part 1: The Real, the Thin and the Thick Lenses*. https://www.thepulsar.be/article/-devoptical-part-1--the-real--the-thin-and-the-thick-lenses/. Accessed: 2022-01-05. 2021.

[7] Noboru Ebizuka et al. "Grisms Developed for FOCAS." en. In: *Publications of the Astronomical Society of Japan* 63.sp2 (Mar. 2011), S613–S622.

[8] *Entrance Optics*. https://www.horiba.com/int/technology/spectroscopy/spectrometers-and-monochromators/entrance-optics/. Accessed: 2022-01-01.

[9] Nicholas James Gregory Hollows. *System Throughput, f/, and Numerical Aperture*. https://www.edmundoptics.com/knowledge-center/application-notes/imaging/lens-iris-aperture-setting/. Accessed: 2022-01-05.

[10] *Grisms: Uses and Advantages*. en. https://wasatchphotonics.com/technologies/grisms-uses-advantages/. Accessed: 2022-1-10. Feb. 2019.

[11] Gary J Hill et al. "Volume phase holographic (VPH) grisms for optical and infrared spectrographs." en. In: *Specialized Optical Developments in Astronomy*. Vol. 4842. SPIE, Jan. 2003, pp. 1–9.

[12] Matthew Jones. *Waves and Oscillations*. http://www.physics.purdue.edu/~jones105/phys42200_Spring2013/notes/Phys42200_Lecture32.pdf. Accessed: 2022-01-05. 2013.

[13] *Lenses*. https://courses.lumenlearning.com/boundless-physics/chapter/lenses/. Accessed: 2022-01-09.

[14] *Monochromator System Optics*. https://www.horiba.com/int/monochromator-system-optics/#c8380. Accessed: 2022-01-01.

[15] Sam Brown N. W. Edmund. *Graphical Ray Tracing*. Edmund Scientific Co. 1968.

[16] Carl R. Nave. *Principal Planes*. http://hyperphysics.phy-astr.gsu.edu/hbase/geoopt/priplan.html. Accessed: 2022-01-05. 2017.

[17] *Paraxial Rays*. http://hyperphysics.phy-astr.gsu.edu/hbase/geoopt/paraxial.html. Accessed: 2022-01-01.

[18] *Part 1: The Slit*. https://bwtek.com/spectrometer-part-1-the-slit/. Accessed: 2022-01-01.

[19] *Resolvance of Grating*. http://hyperphysics.phy-astr.gsu.edu/hbase/phyopt/gratres.html. Accessed: 2022-01-10.

[20] Ruxandra Serbanescu. *Thick Lenses*. https://www.physics.utoronto.ca/~phy224_324/exercises/index-of-refraction/ThickLenses.pdf. Accessed: 2022-01-05. 2013.

[21] *Spectrometer Design Guide*. https://ibsen.com/wp-content/uploads/Spectrometer-design-guide.pdf. Accessed: 2022-01-01. 2017.

[22] *Spectrometer Throughput and Etendue*. https://www.horiba.com/int/technology/spectroscopy/spectrometers-and-monochromators/spectrometer-throughput-and-etendue/. Accessed: 2022-01-01.

[23] *The Slit*. https://www.optecks.com/Portal/index.php/knowledge-center/spectroscopy-root/spect3. Accessed: 2022-01-01.

[24] *Thin Lens Equation*. http://hyperphysics.phy-astr.gsu.edu/hbase/geoopt/lenseq.html. Accessed: 2022-01-01.

[25] *What is a spectrometer slit?* https://www.stellarnet.us/what-is-a-spectrometer-slit/. Accessed: 2022-01-01. 2017.

[26] *Why Use an Achromatic Lens?* https://www.edmundoptics.com/knowledge-center/application-notes/optics/why-use-an-achromatic-lens/. Accessed: 2022-01-09.

[27] Wikipedia contributors. *Snell's law*. https://en.wikipedia.org/wiki/Snell%27s_law. Accessed: NA-NA-NA.

Appendices

The appendix contains all mathematical models relevant to the modelling of the component and system parameters of the payload designer.

A Foreoptics Model

Jennifer

The fore-optics of the spectrometer is the entrance optics, which serves as a telescope. Although its components are unknown, it can be treated as a black box.

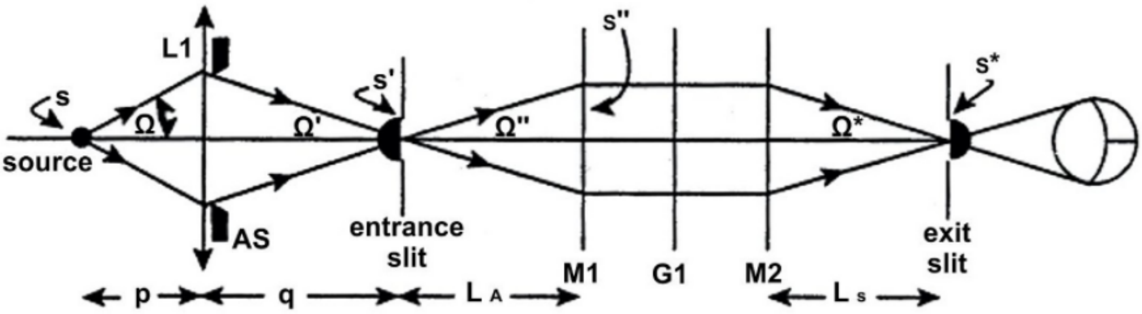

Figure 3: A monochromator system. [22]

S = area of source
S' = area of entrance slit
S" = area of mirror M1
$S*$ = area of exit slit
Ω = half angle of light collected by L1
Ω' = half angle of light submitted by L1
Ω" = half angle of light collected by M1
$\Omega*$ = half angle of light submitted by M2
$L1$ = lens used to collect light from source
$M1$ = spherical collimating Czerny-Turner mirror
$M2$ = spherical focusing Czerny-Turner mirror
AS = aperture stop
LS = illuminated area of lens L1
p = distance from object to lens L1
q = distance from lens L1 to image of object at the entrance slit
$G1$ = diffraction grating

Table 1: Foreoptic component parameters.

Parameter	Symbol	Min	Expected	Max	Unit
Aperture diameter[4]	$d_{aperture}$				mm
Back focal length[5]	BFL				mm
Effective focal length	EFL				mm
F-number	N				-
Image diameter[6]	d_{image}				mm
Mass	m		80		g
Maximum angle of incidence	$\theta_{in,max}$				°
Mechanical length	L	0		100	mm
Numerical aperture	NA				
Spectral transmittance	$T(\lambda)$	0	-	100	%

A.1 Aperture Diameter

A.2 Effective Focal Length

A.3 Telecentricity

should be very important in your system because it has to be matched to your relay / diffraction stage optics otherwise you may end up with severe vignetting. (src: Tymen Nagel from Chromar Technologies)

A.4 Magnification

The magnification of the fore-optics is calculated by [8]:

$$M = \frac{q}{p} \tag{1}$$

Where M is the magnification, q is the image distance from the fore-optic lens, p is the object distance from the fore-optic lens, as seen in Figure 3.

A.5 Numerical Aperture

Numerical Aperture is the light gathering power of an optic, characterizing the range of angles of light rays that can enter or exit an optical component (e.g. lens, slit) [14].

$$NA = \mu \sin \Omega \tag{2}$$

Where μ is the refractive index (1 in air), ω is the angle of the marginal ray from the optical axis (from Figure 3).

The numerical aperture (1/f-number/2) sets the angle of the rays at the edge of the focused cone of energy. This must be tied in with the maximum AOI at the edge of the field (acceptable deviation from perfect telecentricity). This should be considered when determining the first order specifications. (Tymen Nagel from Chromar Technologies)

A.6 Minimum Back Focal Length

A.7 F/value (f/number)

The F value, often known as the f/number, of a lens system is the ratio of the image distance to the diameter of the slit:

$$f/value = \frac{1}{2NA} = \frac{q}{d} \tag{3}$$

Where NA is the numerical aperture, q is the image distance from the fore-optic lens, d is the diameter of the aperture in the fore-optic system. When the object distance is very far (approaches infinity), the image distance is effectively the same as the focal length of the lens.// Note: $NA = sin(\Omega)$, from Figure 3, which approximates to $\frac{1}{2f/number}$ [14].

The f/number is usually set by adjusting the diaphragm/aperture in most lens systems. The lower the lens' f/number, the larger the iris, and more light is able to pass through the system (greater throughput). The f/number usually increases by multiple of $\sqrt{2}$, since the aperture area typically varies by a factor of 2 [9].

A.8 Geometric Etendue

The geometric etendue of an optical system is its ability to accept light, characterized by the maximum beam size the optical component can accept. As such, it can limit light throughput of the spectrometer. It is calculated by [22]:

$$d^2G = \frac{dS}{dQ} \tag{4}$$

[4] A.k.a aperture size.
[5] A.k.a back focal distance.
[6] A.k.a image diagonal.

$$G = \iint \frac{dS}{dQ} \tag{5}$$

Where G is the geometric etendue, S is the area of the emitting source, Q is the solid angle into which light propagates (2Ω in Figure 3). Through integration:

$$G = \pi \Sigma \sin^2 \Omega \tag{6}$$

Where G is the geometric etendue, Ω is the angle of the marginal ray from the optical axis. In order to optimize throughput, the maximum beam size that is acceptable by the optical component should be used, and:

$$G = \pi S \sin^2 \Omega = \pi S' \sin^2 \Omega' = \pi S" \sin^2 \Omega" = \pi S^* \sin^2 \Omega^* \tag{7}$$

A.9 Flux

From the geometric etendue, flux, defined as "energy/time (photons/sec, or watts) emitted from a light source or slit of given area, into a solid angle at a given wavelength (or bandpass)", can be calculated [22]:

$$\phi = B \times G \tag{8}$$

$$\phi = B \pi S' \sin^2 \Omega' \tag{9}$$

Where B is the radiance of the source, S' is the area of the entrance slit or emitting source, Ω' is the angle of the marginal ray from the optical axis; shown in Figure 3.

B Slit Model

Jennifer

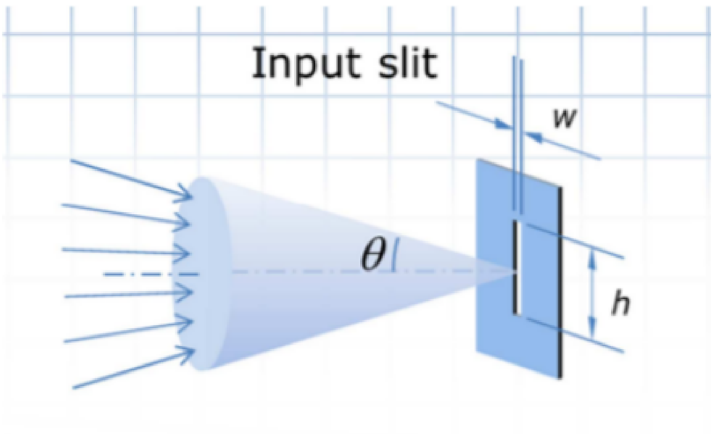

Figure 4: Light arriving at the entrance slit of a spectrometer. [5]

The light output from the fore optics passes through a narrow, vertical slit, which plays a large role in determining the throughput of the optical system (i.e. amount of light, measured by photon flux) and resolution. These are affected by the size (height and width) of the entrance slit, pictured in figure 4. The standard slit height is 1 mm, with options of up to 2 mm available as well [18]. Slit widths range from $5\mu m$ to $800\mu m$, with standard sizes: 10, 14, 25, 50, 100 and 200 μm [25]. It must be placed exactly within the optical path of the spectrometer, its distance from the fore-optics dependent on the image distance from the fore-optic lens [8], and distance from the collimator dependent on the focal point of the collimation lens [21].

Decreasing the slit width blocks incoming light travelling at larger angles, with respect to the optical axis, improving resolution while decreasing light throughput. Therefore, both factors must be taken into consideration when optimizing slit width [23].

B.1 Image Width

The image width of the entrance slit is estimated as [18]:

$$W_i = \sqrt{M^2 \times W_s^2 + W_o^2} \tag{10}$$

Where M is the magnification of the optical bench (i.e. ratio of the focal length of the focusing lens to that of the collimating lens), W_s is entrance slit width, and W_o is object width (in this case, the image broadening from the optical bench).

B.2 Slit Width

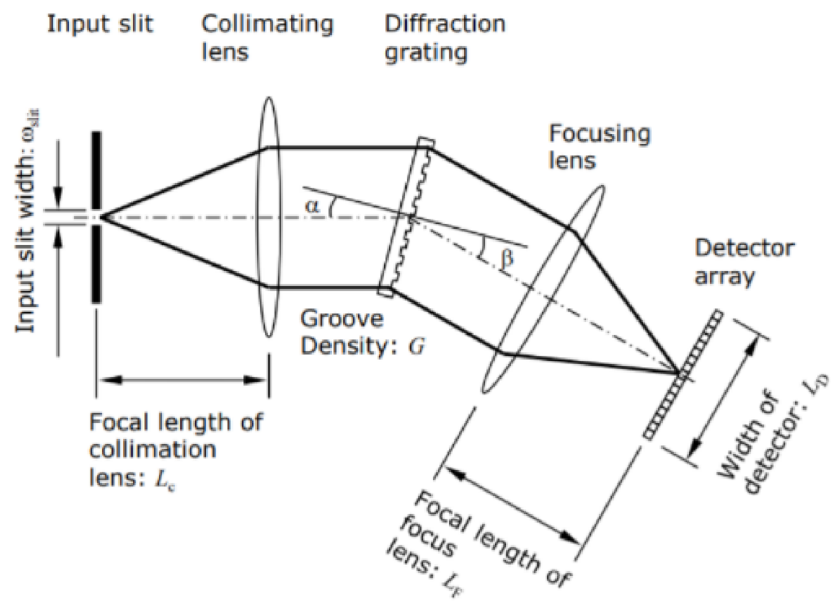

Figure 5: A typical set-up of a spectrometer. [21]

It is suggested to select a slit width after other components have already been selected, since:

$$w_{slit} = \frac{G\Delta\lambda L_c}{\cos\alpha} \tag{11}$$

Where G is the grating groove density, $\Delta\lambda$ is the resolution, L_c is the focal length of the collimator, and α is the angle of incidence, seen in Figure 5.

C Lens Models

The lens models we derive here apply for lenses operating on light which is collimated[7] either on the onset or outset. We focus on these two scenarios because the payload specifically makes use of lenses acting as either *collimators* or *focusers*. A collimator takes a point source of light (i.e. light exiting the slit) and produces a collimated beam. A focuser takes collimated light and produces an image (i.e. the lens responsible for focusing the diffracted light from the diffractor onto the sensor). Despite being a distinguishing factor between candidate models, chromatic aberrations are not taken into account for the reasons noted in section 4.

C.0 Thin Singlet Lens Model

David

A thin lens is a mathematical approximation of a real lens, which typically have non-negligible thickness. For sufficiently thin lenses, however, the thin lens equations are an adequate description of the characteristics of the lens [4].

[7] Collimated light is light whose rays propagate in parallel.

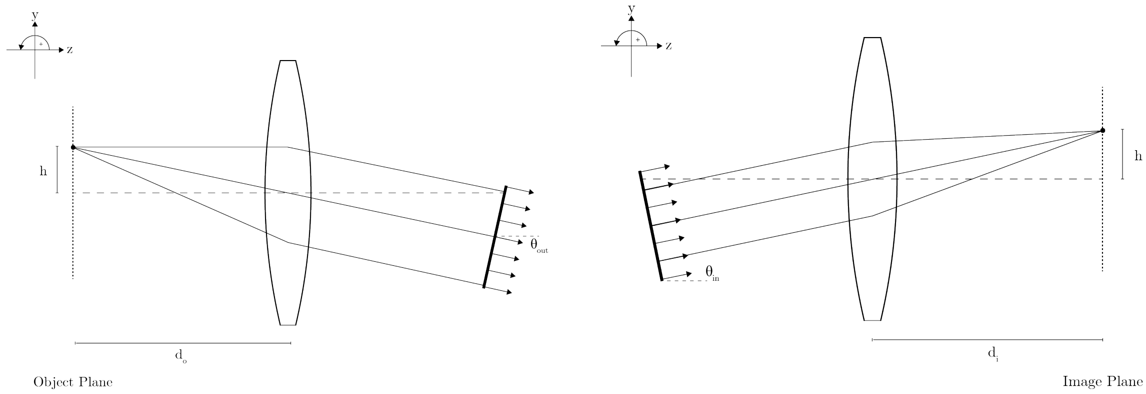

(a) Collimator (b) Focuser

Figure 6: Thin singlet models.

C.0.1 Image distance

The image distance in the case of a thin focuser is the distance between the lens and the image plane. Estimating this distance is accomplished via the thin lens equation [24]:

$$\frac{1}{f} = \frac{1}{d_o} + \frac{1}{d_i} \tag{12}$$

Where f is the focal length of the thin lens, d_o is the distance from the lens to the object or source, and d_i is the distance from the lens to the object's image.

Collimated light is represented by a source that is an infinite distance away. Thus:

$$\lim_{d_o \to \infty} \frac{1}{f} = \frac{1}{d_o} + \frac{1}{d_i} \Rightarrow \frac{1}{f} = \frac{1}{d_i} \tag{13}$$

Rearranging for d_i:

$$\boxed{d_i = f} \tag{14}$$

Assumes:

- Rays are paraxial.[8]
- Lens is of negligible thickness.
- Incoming light is perfectly collimated.

C.0.2 Source distance

Similarly, for a collimator we estimate the source or object distance d_o by assuming the image formed by the lens is an infinite distance away:

$$\lim_{d_i \to \infty} \frac{1}{f} = \frac{1}{d_o} + \frac{1}{d_i} \Rightarrow \frac{1}{f} = \frac{1}{d_o} \tag{15}$$

Solving for d_o:

$$\boxed{d_o = f} \tag{16}$$

Assumes:

- Rays are paraxial.
- Lens is of negligible thickness.
- Incoming light is perfectly collimated.

[8] Paraxial rays are rays of light at small enough angles from the optical axis that they are well described by the small angle approximation [17].

C.0.3 Image height

David

A parallel bundle of rays incident on a focuser will focus at the intersection of the center ray with the focal plane [15, 4]. By trigonometry:

$$\tan(\theta_{in}) = \frac{h}{d_i} \tag{17}$$

$$h = d_i \tan(\theta_{in}) \tag{18}$$

Where h is the height of the point of focus for the ray bundle along the focal plane from optical axis, d_i is the distance of the focal plane from the lens, and θ_{in} is the incoming angle of the collimated rays.

We know from section C.0.1 that for a thin lens, the focal length defines the distance from the lens to the focal plane ($d_i = f$). Thus,

$$\boxed{h = f \tan(\theta_{in})} \tag{19}$$

Assumes:

- Thin lens approximation.
- Does not account for field curvature.[9]

C.0.4 Source Height

Similarly, the source height for a collimator can be found as:

$$\tan(\theta_{out}) = \frac{h}{d_o} \tag{20}$$

$$h = d_o \tan(\theta_{out}) \tag{21}$$

$$\boxed{h = f \tan(\theta_{out})} \tag{22}$$

C.1 Focal length

We can derive the focal length for the thin lens in four ways:

C.1.1 Magnification

The concept of magnification for collimated light does not apply, as linear magnification is undefined. To see why, we begin with the definition of linear magnification [4]:

$$m = \frac{h_i}{h_o} = -\frac{d_i}{d_o} \tag{23}$$

Where m is the linear magnification, h_i is the image height, h_o is the object height, d_i is the image distance from the lens, and d_o is the object distance from the lens. Taking the limit as d_i or d_o go to infinity yields an undetermined magnification.

C.2 Thick Singlet Model

Stephanie

[9] Field curvature is a type of optical abberation in which a flat object normal to the optical axis cannot be brought properly into focus on a flat image plane, but instead the focal plane ends up curved.

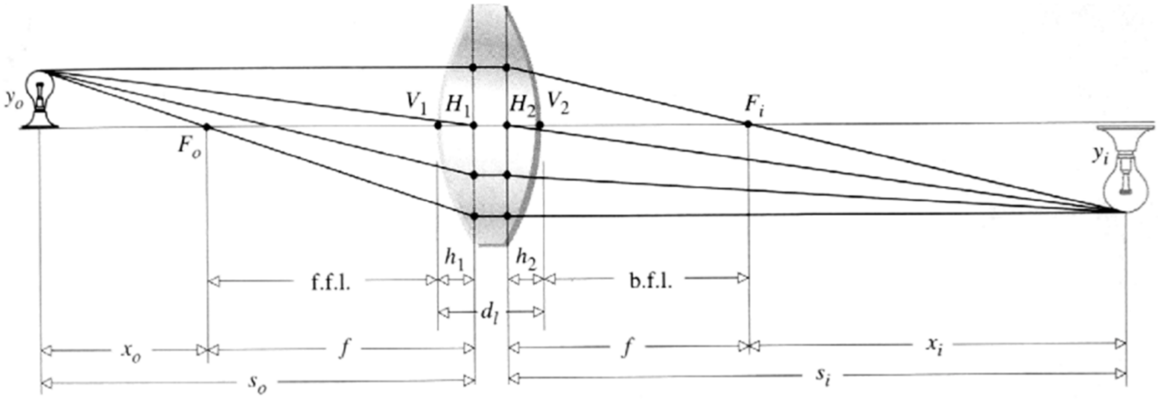

Figure 7: The thick lens model [12].

C.2.1 Position of the principal planes

A thick lens is a lens whose thickness is not negligible. Therefore, we have to consider the refraction of a light ray at both surfaces of the thick lens (i.e., the image formed by the first surface is treated as the object for the second surface).

To compute the position of the image of an object at a given distance from the thick lens, we need to calculate the position of the principal planes of the thick lens. All refraction is considered to occur at the principal planes and for a given lens, the principal planes do not depend on object position [16].

For a bispherical lens:

- Position of the first (or primary) principal plane [16]:

$$h_1 = -\frac{f(n-1)d}{R_2 n} \tag{24}$$

- Position of the second (or secondary) principal plane [16]:

$$h_2 = -\frac{f(n-1)d}{R_1 n} \tag{25}$$

Where h_1 and h_2 are the distances between the vertices of the lens and the principal planes, f is the focal length of the lens, n is the index of refraction of the lens, and d is the thickness of the lens (i.e., the distance between the two vertices of the lens).

R_1 and R_2 are the radii of curvature of the thick lens. If the vertex of the lens surface lies in front of the centre of curvature of that surface, the radius of curvature is positive. If the vertex lies behind the centre of curvature, the radius of curvature is negative [20]. (E.g. in Figure 7, the front (left) surface has positive radius of curvature while the back (right) surface has negative.)

These equations assume that the light rays are close to the optical axis (i.e., in the paraxial region). Away from the paraxial region, the principal planes bend as spheres instead [6].

C.2.2 Focal length

The Lensmaker's equation calculates the focal length of a thick lens in air ($n_m = 1$) [12, 13, 16]:

$$\frac{1}{f} = (n-1)\left(\frac{1}{R_1} - \frac{1}{R_2} + \frac{(n-1)d}{nR_1R_2}\right) \tag{26}$$

Rearranging for f:

$$f = \frac{nR_1R_2}{(R_2 - R_1)(n-1)n + (n-1)^2 d} \tag{27}$$

For a thick lens in a medium []:

$$\frac{1}{f} = \frac{n_l - n_m}{n_m}\left(\frac{1}{R_1} - \frac{1}{R_2} + \frac{n_l - n_m}{n_m} \cdot \frac{d}{n_l R_1 R_2}\right) \tag{28}$$

Rearranging for f:

$$f = \frac{n_m^2 n_l R_1 R_2}{(R_2 - R_1)(n_l - n_m)n_m n_l + (n_l - n_m)^2 d} \tag{29}$$

Where f is the focal length of the lens, n_l is the index of refraction of the lens, n_m is the index of refraction of the medium surrounding the lens, d is the thickness of the lens (i.e., the distance between the two vertices of the lens), and R_1 and R_2 are the radii of curvature of the thick lens.

Both equations assume that the medium on both sides of the lens have the same index of refraction. Therefore, the focal lengths from the two principal planes are equal [20].

C.2.3 Image distance from principal plane

For a thick lens, we use the same equation as the thin lens to calculate image distance [12]:

$$\frac{1}{f} = \frac{1}{s_o} + \frac{1}{s_i} \tag{30}$$

Rearranging for s_i:

$$s_i = \frac{s_o f}{s_o - f} \tag{31}$$

Where f is the focal length of the thick lens, s_o is the distance from the object to the first principal plane, and s_i is the distance from the second principal plane to the image.

C.2.4 Image distance from focal point

To calculate the image distance from the focal point [12]:

$$f^2 = x_o x_i \tag{32}$$

Rearranging for x_i:

$$x_i = \frac{f^2}{x_o} \tag{33}$$

Where f is the focal length of the thick lens, x_o is the distance from the object to the first focal point, and x_i is the distance from the second focal point to the image.

C.2.5 Image height

The height of the image produced by a thick lens can be calculated using the magnification of the lens [12]:

$$m_T = -\frac{s_i}{s_o} = \frac{h_i}{h_o} \tag{34}$$

Rearranging for h_i:

$$h_i = m_T h_o = -\frac{h_o s_i}{s_o} \tag{35}$$

Where m_T is the magnification of the lens, s_o is the distance from the object to the first principal plane, s_i is the distance from the second principal plane to the image, h_o is the height of the object, and h_i is the height of the image.

C.3 Achromatic Doublet Model

Amy

An achromatic doublet is composed of two elements: a concave lens (made of flint glass, which has a high refractive index) and a convex lens (made of crown glass, which has a low refractive index) [26].

Chromatic aberration is the effect caused by the difference in refractive index for a given material at different wavelengths. This can be reduced by an achromatic doublet as its two lenses compensate for their respective dispersions. Other types of aberration include coma and spherical aberration, which can be corrected for by the optimization process described in the following sections [1].

C.3.1 Choosing materials for each lens

An Abbe diagram can be used to choose the two glass types for the achromatic doublet with the following taken into consideration:

- The crown glass should have a higher Abbe number than the flint glass
- The flint glass should have a higher refractive index than the crown glass
- A large difference in Abbe numbers will help optimize coma and spherical aberrations

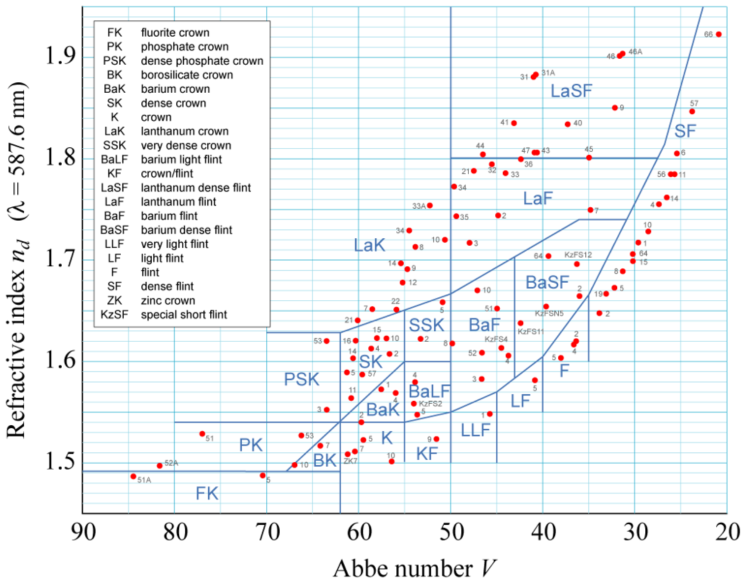

Figure 8: Abbe diagram [1]

C.3.2 Calculating focal lengths of lens pair

The achromatic doublet can be approximated as a linear system:

$$\frac{1}{f_1} + \frac{1}{f_2} = \frac{1}{f_{eq}} \tag{36}$$

where f_1 and f_2 are the focal lengths of the first and second element respectively and f_eq is the effective focal length of the entire system. Furthermore,

$$\frac{1}{f_1 V_1} + \frac{1}{f_2 V_2} = 0 \tag{37}$$

where V_1 and V_2 are the Abbe numbers for the first and second elements respectively.

<u>Note:</u> A typical Abbe number for crown glass is about 0.016 and a typical Abbe number for flint glass is about 0.028.

Combining (36) and (37):

$$f_1 = \frac{V_1 - V_2}{V_1} f_{eq} \tag{38}$$

$$f_2 = -\frac{V_1 - V_2}{V_2} f_{eq} \tag{39}$$

C.3.3 Calculating effective focal length

Both (38) and (39) can be rearranged to derive the effective focal length f_eq as a function of either f_1 or f_2:

$$f_eq = f_1 \frac{V_1}{V_1 - V_2} \tag{40}$$

$$f_eq = -f_2 \frac{V_2}{V_1 - V_2} \tag{41}$$

C.3.4 Calculating radius of curvature

Assuming symmetric lenses with equal radii of curvature in the front and back surfaces of each lens, the radii of curvature for each lens denoted R_1 and R_2 can be found using the following:

$$R_1 = 2f_{eq} \frac{V_1 - V_2}{V_1} (n_1 - 1) \tag{42}$$

$$R_2 = 2f_{eq} \frac{V_2 - V_1}{V_2} (n_2 - 1) \tag{43}$$

where n_1 and n_2 are the refractive indices of the materials.

D Dichroic Bandpass Filter Model

Eman

A Dichroic Bandpass Filter uses dielectric layers on glass that transmit a desired range of wavelengths, and reflects the rest. These filters can be categorized into single-cavity and multi-cavity, based on the model.

D.1 Incident Beam

The phase shift of a non-normal incident beam is represented by the following equation:

$$\lambda_\theta = \lambda_0 \times \sqrt{1 - (\frac{n_0}{n^*} sin\theta)^2 (44)}$$

Where:
λ_θ = the wavelength of the beam at angle of incidence θ
λ_0 = the wavelength of the beam at normal incident angle
n_0 = refractive index of the incident medium
n^* = effective refractive index of the bandpass filter

Although the filter is made of multiple layers with different indices of refraction, calculations can be done using the effective refractive index, which has a value that is between the highest and lowest indices of the filter layers.

The effective refractive index is represented by the following equation:

$$(n^*)^2 = \frac{(0.5A + k\pi)}{\frac{0.5A}{n^2} + 2J} \tag{45}$$

Where:

$$A = (\epsilon_1^0 + \epsilon_2^0 + N\pi) \tag{46}$$

n = refractive index of spacer layer

$$k\pi = the\ frequency\ term,\ which\ depends\ on\ the\ type\ of\ stack. \tag{47}$$

There are 3 types of stacks to consider:

- Symmetrical, where the beam is incident on the layer with high index.
- Asymmetrical, where the beam is incident on the layer with high index.
- Asymmetrical, where the beam is incident on the layer with low index.

$$J = \frac{\delta_\epsilon}{\delta(\sin^2 \phi_e)} \tag{48}$$

D.2 Transmitted Beam

According to Pidgeon and Smith, the

$$T = \frac{T_1(\omega) T_2(\omega)}{1 - R\omega}^2 \tag{49}$$

Where:
$\mathrm{T}_1, T_2 are the transmittances of the system$
$R_1, R_2 are the reflectances of the system$

E Diffractor Models

E.1 Surface-Relief Grating Model

Ginny

Surface relief gratings have been descoped for the payload due to their low diffraction efficiency relative to VPH gratings, but are implemented to form a numerical baseline for performance comparison.

The surface relief model considered is the transmission diffraction grating mode, where the diffracted rays lie on the opposite side of the grating from the incident rays. Each grating groove can be pictured as being a small, slit-shaped source of diffracted light.

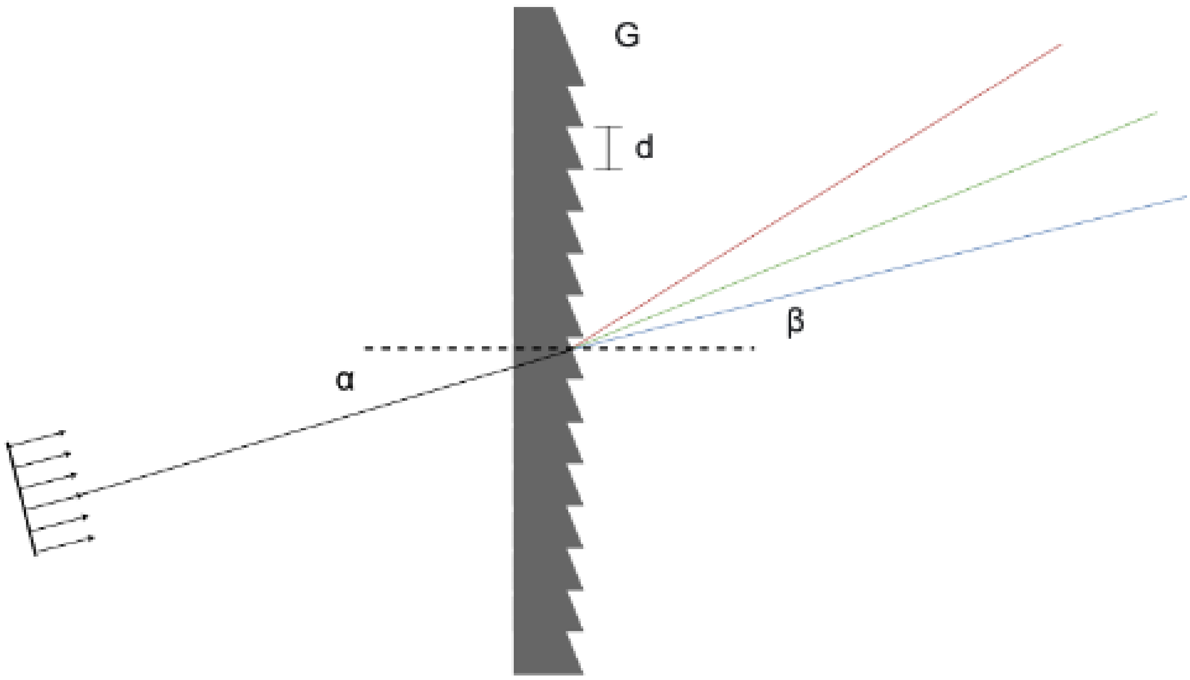

Figure 9: The VPH grism model diagram.

Figure x visualizes the diffraction of a beam of monochromatic light as it passes through a transmission grating and disperses the light spatially by wavelength λ, where α is the incident angle, β is angle of the diffracted rays exiting the grating, on the opposite side, and d is the groove spacing of the grating.

The relationships can be expressed by the grating equation:

$$Gm\lambda = sin\alpha + sin\beta \tag{50}$$

Where $G = 1/d$ is the groove density of the transmission diffraction grating, and m is the diffraction order (or spectral order) which will be taken as 1. Therefore, to isolate for the angular locations of the principle intensity maxima when light of wavelength λ is diffracted from a grating of groove density G at an order of $m = 1$:

$$\beta = arcsin(G\lambda - sin\alpha) \tag{51}$$

E.1.1 Dispersion

Angular dispersion of a grating is a function of the angles of incidence and diffraction, the latter of which is dependent upon groove spacing. Angular dispersion can be increased by increasing the angle of incidence or by decreasing the distance between successive grooves. A grating with a large angular dispersion can produce good resolution in a compact optical system. Angular dispersion is the slope of the curve given by $\lambda = f(\theta)$. In auto collimation, the equation for dispersion is given by:

$$\frac{d\lambda}{d\theta} = \frac{lambda}{2tan\theta} \tag{52}$$

E.1.2 Resolving Power and Spatial Resolution

The resolving power R of a grating is a measure of its ability to separate adjacent spectral lines of average wavelength λ. It can be expressed as follows:

$$R = \frac{W(sin\alpha + sin\beta)}{\lambda} \tag{53}$$

where W is the ruled width of the grating.

The relationship shows that the degree to which the theoretical resolving power is attained depends not only on the angles α and β, but also the optical quality of the grating surface, the uniformity of the groove spacing, the quality of the associated optics in the system, and the width of the slits. The groove spacing must be kept constant to within about one percent of the wavelength at which theoretical performance is desired. Experimental details, such as slit width, air currents, and vibrations and seriously interfere with the diffraction mechanism.

E.2 VPH Grating Model

Ginny

A volume phase holographic grating consists of a dichromate gelatin (DCG) film between two glass substates. It is designed to reduce periodic error that can occur in blazed gratings, having a high 1st order diffraction peak frequency, low polarization dependence, and uniform performance over broad bandwidths.

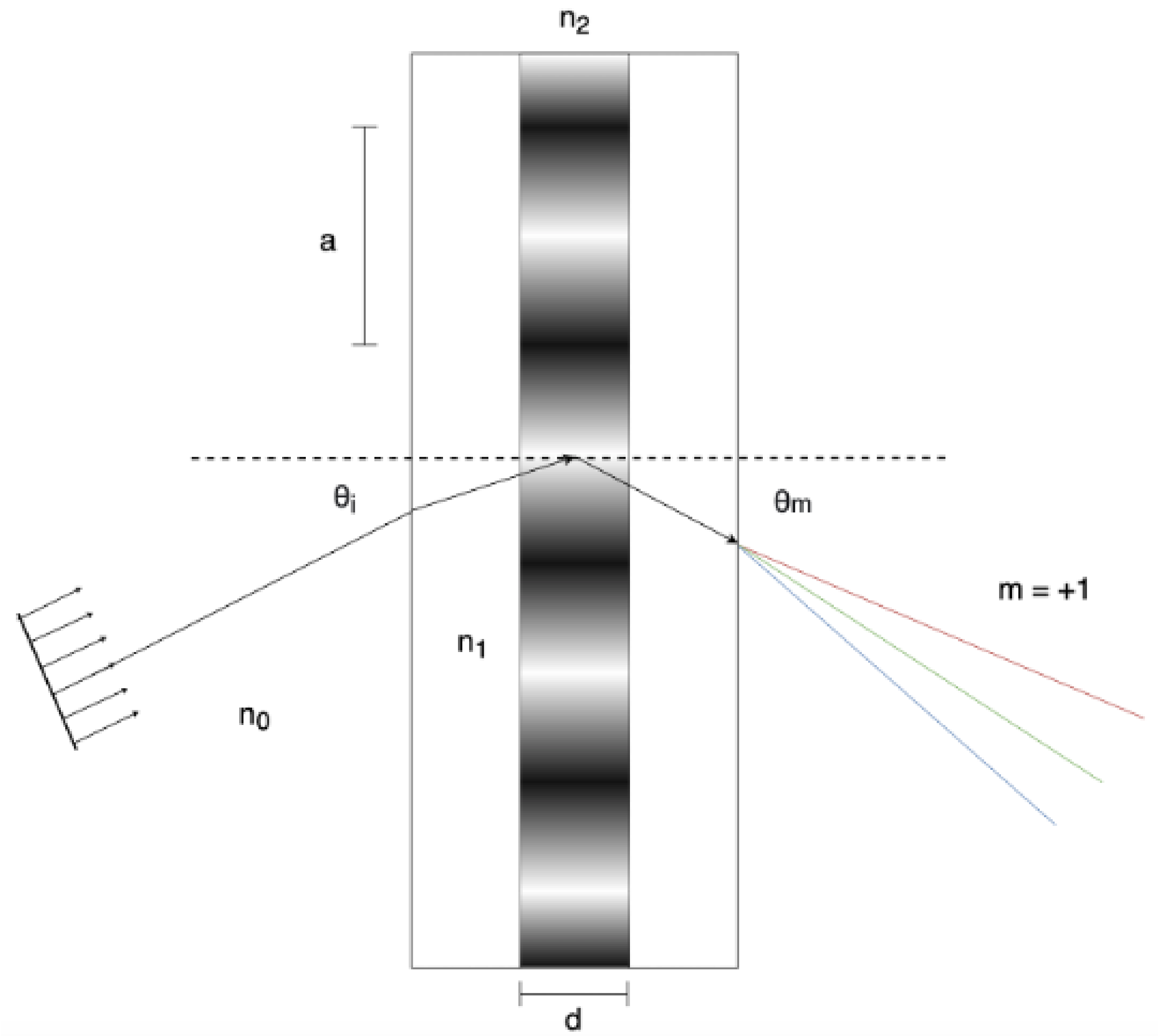

Figure 10: The VPH grism model diagram.

Figure x shows the geometry and variables of a VPH grating, where d is the film thickness, n_2 is the bulk index (average index of refraction between Gragg planes).

The light passing through a VPH grating obeys a similar relationship to a surface-relief diffraction grating, given by

$$\frac{m\lambda}{n_i} = \Lambda_g(sin\alpha_i + sin\beta_i) \tag{54}$$

where m is an integer (the spectral order), l is the wavelength in vacuum, n_i is the refractive index of the medium, Λ_i is the grating period (which is the projected separation between the fringes in the plane of the grating, equivalent to the groove spacing on a ruled grating), α_i is the angle of incidence, and β_i is the angle of diffraction from the grating normal.

E.3 VPH Grism Model

Kejsi, David

A grism is a compound optical element composed of a diffraction grating sandwiched between prisms [10].

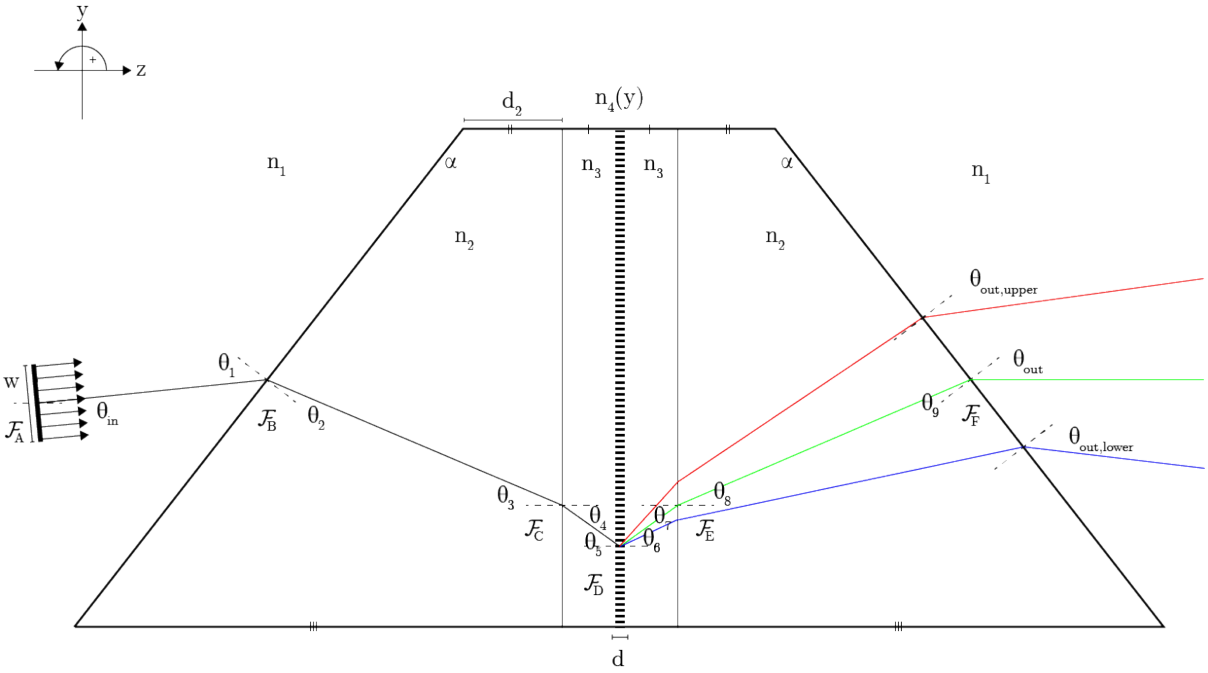

Figure 11: The VPH grism model diagram.

Where n_1, n_2, and n_3 are the indices of refraction of the external medium, prism medium, and VPH hermetic seal medium, respectively. n_4 is the sinusoidally-varying index of refraction of the dichromated gelatin material of the VPH grating.

E.3.1 Angular distribution of diffracted wavelengths

David

An important parameter that defines the performance of a grism is the angular distribution of diffracted wavelengths. This is, in other words, a mapping between the wavelengths produced by the diffractor and the angles those wavelengths leave the component. To solve for this mapping, we observe a bundle of collimated light entering the grism at some angle and successively apply Snell's law at every interface and the diffraction equation at the grating surface. We begin as:

$$\theta_1 = \theta_{in} + \alpha \tag{55}$$

Where α is the apex angle of the prisms. In this model, the prisms are assumed to be symmetrical, but they need not be. A symmetrical grism is typically shorter height-wise compared to a non-symmetrical grism [11], so is pursued in this design. By Snell's law [27]:

$$n_1 \sin(\theta_1) = n_2 \sin(\theta_2) \tag{56}$$

$$\theta_2 = \arcsin\left(\frac{n_1}{n_2}\sin(\theta_1)\right) \tag{57}$$

$$\theta_3 = \alpha - \theta_2 \tag{58}$$

$$\theta_4 = \arcsin\left(\frac{n_2}{n_3}\sin(\theta_3)\right) \tag{59}$$

$$\theta_5 = \theta_4 \tag{60}$$

A VPH grating diffracts light according to the standard grating equation in the same manner as a classical surface-relief grating, represented by [2, 3]:

$$m\nu\lambda = \sin(\alpha) - \sin(\beta) \tag{61}$$

where m is the order of diffraction, ν is the grating frequency, λ is the wavelength of light of interest, α is the angle of incidence, and β is the angle of diffraction of this wavelength [2, 3]. Hence:

$$\begin{aligned} m\nu\lambda &= \sin(\theta_5) - \sin(\theta_6) && (62) \\ \sin(\theta_6) &= \sin(\theta_5) - m\nu\lambda && (63) \\ \theta_6 &= \arcsin(\sin(\theta_5) - m\nu\lambda) && (64) \end{aligned}$$

$$\theta_7 = \theta_6 \tag{65}$$

$$\theta_8 = \arcsin\left(\frac{n_3}{n_2}\sin(\theta_7)\right) \tag{66}$$

$$\theta_9 = \theta_8 - \alpha \tag{67}$$

$$\theta_{10} = \arcsin\left(\frac{n_2}{n_1}\sin(\theta_9)\right) \tag{68}$$

Thus,

$$\boxed{\theta_{out} = \theta_{10} + \alpha} \tag{69}$$

Assumes:

- Angles are small enough or grism is large enough that rays intersect all surfaces of the grism.[10]

E.3.2 Undeviated wavelength

David

The undeviated wavelength is the wavelength which exits the grating at an angle equal and opposite to the angle of incidence with respect to the grating surface normal, in such a way as:

$$\alpha = -\beta \tag{70}$$

Where α is the angle of incidence, and β is the angle of diffraction. Equation (61) can then be simplified as follows:

$$m\nu\lambda = \sin(\alpha) - \sin(-\alpha) \tag{71}$$

By negative angle identity:

$$m\nu\lambda = 2\sin(\alpha) \tag{72}$$

$$\boxed{\lambda_g = 2\frac{\sin(\alpha)}{m\nu}} \tag{73}$$

Where λ_g is the undeviated wavelength. Equation (73) is a simplified form of the Bragg condition, which assumes the grating fringes are normal to the grating surface [3].

E.3.3 Diffraction Efficiency

Kejsi

For a transmission VPH grating with fringe structure normal to the grating surface, the diffraction efficiency for the two planes of polarization can be estimated by

$$\eta_s = \sin^2\left(\frac{\pi\Delta n_g d}{\lambda\cos(\alpha_g)}\right) \tag{74}$$

$$\eta_p = \eta_s\cos(\alpha_g + \beta_g) \tag{75}$$

[10] In other words, no light escapes the grism prematurely.

Check if above assumes bragg condition.
where η_p is the diffraction efficiency with respect to the plane of incidence
in which and are the angles of incidence and diffraction within the grating volume [3].
This equation is valid when the following equation is satisfied:

$$Q = \frac{2\pi\lambda d}{n_g \lambda^2} > 10 \tag{76}$$

E.3.4 Resolvance

Kejsi

Resolvance or resolving power is a common way of expressing resolution for a grating.Grisms can range from low to high resolving powers, typically in the range of 280 to 8200 [7]. Diffraction gratings have multiple grooves that follow the same relations as a double slit. The expression for resolving power of a grating is derived by using the intensity expression for a double slit grating.

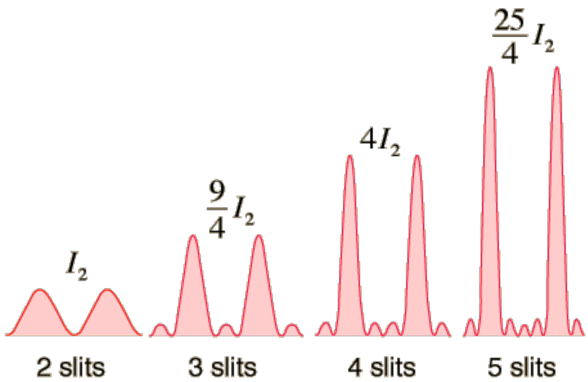

Figure 12: The intensity curves for gratings with varying numbers of slits. Increasing the slits improves the resolution by sharpening the intensity curves.

The peaks have a phase difference of $\delta = 2m\pi$. The closest minimums occur $\frac{\pi}{2}$ away from the peak, which occurs for a phase change of:

$$\Delta\delta = \frac{2\pi}{N} \tag{77}$$

Where N is the number of slits.

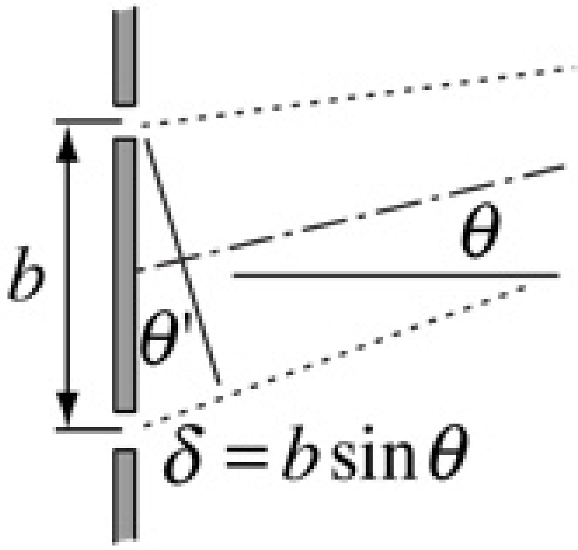

Figure 13: A two-slit grating showing the parameters b, θ, and δ

From the figure,

$$\delta = \frac{2\pi}{\lambda} b \sin\theta \tag{78}$$

The differential of the above is:

$$d\delta = \frac{2\pi}{\lambda} b \cos\theta d\theta \tag{79}$$

The maximum condition is:

$$b \sin\theta = m\lambda \tag{80}$$

With the differential:

$$b \cos\theta d\theta = m d\lambda \tag{81}$$

Substituting both differentials gives:

$$\frac{2\pi}{N} = \frac{2\pi}{\lambda} m d\lambda \tag{82}$$

This simplifies to the final resolving power formula:

$$R = \frac{\lambda}{\Delta\lambda} = mN \tag{83}$$

Where λ is the wavelength of interest, $\Delta\lambda$ is the resolution and m is the diffraction order [19].

E.3.5 Resolution

Kejsi

Spatial resolution is size of the smallest feature that can be detected in an image by a sensor due to the detail in the pixels. Spectral resolution is the spectral detail in a band, or the width of each band in the dataset. Spectral resolution is inversely proportional to slit width, groove density and diffraction order. The number of slits, N, can be written as

$$N = n \cdot w \tag{84}$$

where n is the groove density of the grating and w is the slit width.

The expression for spectral resolution can then be written as:

$$\Delta\lambda = \frac{\lambda}{m \cdot n \cdot w} \tag{85}$$

F Sensor Model

F.1 Signal-to-Noise

Table 2: The environmental parameters used to build transmission model A using MODTRAN.

Parameters	Value
Platform Altitude	
Geographic Area	
Ground Type	
Weather Condition	
CO_2 Mixing Ratio	
Waveband	
Solar Altitude Angle	
Surface Albedo	

$$SNR = \frac{s_{target}}{\sigma_{noise}}$$

(86)

F.2 Frequency-Based Signal-to-Noise

G Scrap

Table 3: Typical values for grism model parameters [2].

Parameter	Min	Typical	Max	Unit
η_2	-	1.5	-	-
$\Delta\eta_2$	0.02	-	0.1	-
d	4	-	20	µm
ν	300	-	6000	$\mathrm{L\,mm^{-1}}$